

Bimodal $\text{Co}_{0.5}\text{Zn}_{0.5}\text{Fe}_2\text{O}_4$ /PANI nanocomposites: Synthesis, formation mechanism and magnetic properties

Sanjeev Kumar^a, Vaishali Singh^{a,*}, Saroj Aggarwal^a, Uttam Kumar Mandal^b, Ravinder Kumar Kotnala^c

^aUniversity School of Basic and Applied Sciences, GGS Indraprastha University, Kashmere Gate, Delhi 110 403, India

^bUniversity School of Chemical Technology, GGS Indraprastha University, Kashmere Gate, Delhi 110 403, India

^cNational Physical Laboratory, New Delhi 110 012, India

ARTICLE INFO

Article history:

Received 11 April 2009

Received in revised form 5 October 2009

Accepted 17 October 2009

Available online 22 October 2009

Keywords:

A. Nanocomposites

A. Polymers

A. Nanofibers

B. Magnetic properties

D. Transmission electron microscopy

ABSTRACT

$\text{Co}_{0.5}\text{Zn}_{0.5}\text{Fe}_2\text{O}_4$ /PANI nanocomposites with bimodal size distribution were synthesized via reverse microemulsion method. Structural characterization was done by Fourier transform infrared spectroscopy, X-ray diffraction and transmission electron microscopy. Vibrating sample magnetometer measurement confirmed the ferromagnetic behavior of nanocomposite with saturation magnetization of 3.95 emu/g and low coercive force (39 Oe). It was observed that on nanocomposite formation with PANI nanofibers, $\text{Co}_{0.5}\text{Zn}_{0.5}\text{Fe}_2\text{O}_4$ ferrite nanocrystals undergo transition from being superparamagnetic to ferromagnetic. A mechanistic description of the process has also been presented in view that the process could be extended for the fabrication of other bimodal nanocomposites

1. Introduction

Polyaniline (PANI) is the most extensively studied conductive polymer due to its relatively facile processability and excellent environmental stability, combined with relatively high levels of electronic conductivity as well as thermoelectric and optical properties [1]. The fabrication of 1D polyaniline with nanometer dimensions have attracted intensive interest because they possess dual advantage of being low-dimensional system along with having potential applications like polymeric conducting molecular wires, chemical sensors, biosensors, catalysts, etc. [2–8].

Magnetic nanoparticles with single domain are known to exhibit unique properties such as enhanced magnetic moments, exchanged-coupled dynamics, quantization of spin waves and giant magneto resistance leading to new potential applications in permanent magnets, data storage devices, targeted drug delivery [9–12]. Ferrite nanocrystals are emerging as promising candidates for biomedical and technological applications due to superparamagnetism, enhanced anisotropy and reactive surfaces [11,12]. Keeping this in view the hybrid composite fabricated from ferrite nanocrystals and conductive PANI holds promise of an important class of materials [13,14].

With the advancement in nanoscience and nanotechnology research efforts have now been focused on synthesizing new type of bifunctional nanocomposites with controllable shapes, sizes and assemblages, with new and tunable properties useful for a wide range of applications as this would combine the advantage of the inorganic materials and the organic polymers, otherwise which are difficult to obtain from individual components. This synergetic behavior makes nanocomposite hold broad technological applications [15,16].

Intensive efforts have been devoted to develop techniques for the synthesis of nanocomposites; some of them are electrode deposition [17], in situ polymerization [18], electrochemical synthesis [19], anodic oxidation [20] etc. However only limited approaches have been used to develop simple, mild and efficient route to tune the properties of multicomponent ferrite/PANI nanocomposites [21].

Recently reverse microemulsion polymerization has emerged as an useful strategy for the fabrication of polymer-inorganic nanocomposites [22]. The microemulsion technique allows control of both shape and size via the structure of the surfactant assemblies. Most of the research groups have studied Fe_3O_4 /PANI nanocomposites [23–25] however, a very few reports have dealt with multicomponent ferrite/polyaniline nanocomposites [21,26]. To the best of our knowledge there is no report focusing on the synthesis of $\text{Co}_{0.5}\text{Zn}_{0.5}\text{Fe}_2\text{O}_4$ /PANI nanocomposites by reverse microemulsion route.

The present study is focused on the above-outlined hypothesis driven synthesis of highly monodisperse $\text{Co}_{0.5}\text{Zn}_{0.5}\text{Fe}_2\text{O}_4$ ferrite

nanocrystals and $\text{Co}_{0.5}\text{Zn}_{0.5}\text{Fe}_2\text{O}_4/\text{PANI}$ nanocomposites via reverse microemulsion techniques. The objective of the present study was to investigate the alignment of $\text{Co}_{0.5}\text{Zn}_{0.5}\text{Fe}_2\text{O}_4$ ferrite nanocrystals vis-à-vis PANI nanofibers. The effect of polyaniline on magnetic properties of the nanocomposite was investigated. The structural characterizations were carried out by FTIR, TEM and XRD and magnetic properties were studied through VSM.

2. Experimental section

2.1. Synthesis of the $\text{Co}_{0.5}\text{Zn}_{0.5}\text{Fe}_2\text{O}_4$ ferrite nanocrystals by reverse microemulsion process

In reverse microemulsion route a quaternary system of kerosene/CTAB/isoamylalcohol/ H_2O was selected. For $\text{Co}_{0.5}\text{Zn}_{0.5}\text{Fe}_2\text{O}_4$ ferrite, aqueous solution was prepared by mixing stoichiometric amounts of 0.5 M FeCl_3 , 0.125 M $\text{CoCl}_2 \cdot 6\text{H}_2\text{O}$ and 0.125 M ZnCl_2 . All chemicals used were of analytical grade. Two reverse microemulsion ME_1 and ME_2 were prepared. CTAB (16.67 wt%) was added to kerosene (38.88 wt%) giving a murky emulsion. 11.11 wt% of aqueous solution containing the precursor salts and 11.11 wt% of iso-amyl alcohol were then added to the emulsion under magnetic stirring. The murky emulsion became transparent. The stirring was continued for 1 h resulting in a stable reverse microemulsion (ME_1). Reverse microemulsion (ME_2) was prepared with 0.5 M aqueous solution of NaOH as water phase under similar conditions.

The reverse microemulsion ME_2 was then heated to 80 °C and to this was added reverse microemulsion ME_1 dropwise under constant magnetic stirring. Appearance of blackish brown color after few minutes marks the completion of the reaction and formation of the desired ferrite colloidal solution. The reaction mixture was further stirred for 4 h on magnetic stirrer with temperature maintained at 80 °C. The pH of the reaction was maintained at 12. The nanocrystals present inside the colloid were then collected by centrifugation (10,733g, 20 min). To ensure complete removal of the surfactant, the powder was subjected to several cycles of washing by methanol and double distilled water followed by centrifugation and finally dried in vacuum oven at 100 °C for 48 h.

2.2. Synthesis of PANI nanostructures by reverse microemulsion process

For PANI synthesis, a stable reverse microemulsion (ME_3) with following composition was prepared: 52.52 wt% cyclohexane + 20.24 wt% CTAB + 13.54 wt% aniline and dopant solution + 13.70 wt% iso-amyl alcohol. Second reverse microemulsion (ME_4) was prepared under similar conditions with 1 M aqueous solution of the initiator ammonium per sulphate in place of aniline. The homogeneous reverse microemulsion solution ME_4 was then added dropwise to reverse microemulsion ME_3 under constant stirring at room temperature and the mixture was further stirred for 24 h under inert atmosphere. Protonated emeraldine formation was confirmed by appearance of green color. After 24 h of stirring the resulting content was centrifuged at 5000 rpm to obtain the polyaniline nanostructures followed by washing with methanol and double distilled water several times. The product obtained was dried in a vacuum oven at 50 °C for 48 h.

2.3. Synthesis of $\text{Co}_{0.5}\text{Zn}_{0.5}\text{Fe}_2\text{O}_4/\text{PANI}$ nanocomposites by reverse microemulsion process

To prepare the composite, 0.005 g of magnetic $\text{Co}_{0.5}\text{Zn}_{0.5}\text{Fe}_2\text{O}_4$ ferrite nanocrystals were dispersed in aniline containing reverse microemulsion ME_3 and same procedure was followed as described above for the synthesis of PANI nanostructures. Finally the resulting $\text{Co}_{0.5}\text{Zn}_{0.5}\text{Fe}_2\text{O}_4/\text{PANI}$ nanocomposites were separated by subse-

quent centrifugation followed by washing with methanol and double distilled water and then dried in a vacuum oven at 50 °C for 48 h.

3. Results and discussion

3.1. Structure and morphology

X-ray diffraction was used for structural determination of the as prepared $\text{Co}_{0.5}\text{Zn}_{0.5}\text{Fe}_2\text{O}_4$ ferrite nanocrystals, Fig. 1a. All the peaks of the XRD spectra could be readily indexed to the spinel phase and no characteristic peaks of impurities were detected, confirming the formation of the cubic spinel structure of $\text{Co}_{0.5}\text{Zn}_{0.5}\text{Fe}_2\text{O}_4$ ferrite [27], [JCPDS file no. 79-1150]. The diffraction peaks at 2θ values of 30.9°, 36°, 44.7°, 52.099°, 57° and 63.4° could be ascribed to the reflections of (2 2 0), (3 1 1), (4 0 0), (4 2 2), (5 1 1) and (4 4 0) planes of the $\text{Co}_{0.5}\text{Zn}_{0.5}\text{Fe}_2\text{O}_4$ ferrite nanocrystals, respectively. The lattice constant (a_0) for $\text{Co}_{0.5}\text{Zn}_{0.5}\text{Fe}_2\text{O}_4$ nanocrystals was found to be 8.3561 Å, which is in agreement with the reported literature value [27,28]. The average diameter of the $\text{Co}_{0.5}\text{Zn}_{0.5}\text{Fe}_2\text{O}_4$ ferrite nanocrystals calculated from the broadening of the XRD peak intensity after $K_{\alpha 2}$ corrections using the Debye-Scherrer equation [29] using (3 1 1) peak was 5 nm, which was in close agreement with the TEM results.

The polyaniline nanostructures had also been subjected to X-ray diffraction analysis at 30 °C. Fig. 1b shows the XRD patterns of the resultant polyaniline nanostructures. Broad diffraction peaks centered at $2\theta = 20.7^\circ$ and 25.9° (d -spacing = 4.3 and 3.5 Å respectively) can be ascribed to the periodicity parallel and perpendicular to the polymer chain [30]. It indicated that the resulting polymer was in the form of highly doped emeraldine salt and had good crystallinity [31,32]. Fig. 1c represents the XRD pattern of $\text{Co}_{0.5}\text{Zn}_{0.5}\text{Fe}_2\text{O}_4/\text{PANI}$ nanocomposites revealing a diffused broad amorphous halo over the 2θ range of 10–30° and broad reflections around 15°, 21° corresponding to large molecular weight polyaniline. The presence of diffused broad peaks indicates lower crystalline order owing to the formation of larger fraction of PANI [33]. The preponderance of amorphous peaks of PANI indicates that the crystalline behavior of ferrite is suppressed due to the presence of large fraction of PANI in comparison to ferrite nanocrystals. The results obtained are consistent with the ones obtained by other research groups [25]. The presence of broad reflection around 2θ value of 26° indicates planar configuration of polyaniline due to the densely packed phenyl rings and thus an extensive interchain pie-pie orbital overlap [31]. This peak is present in the XRD spectra of both pure PANI as well as

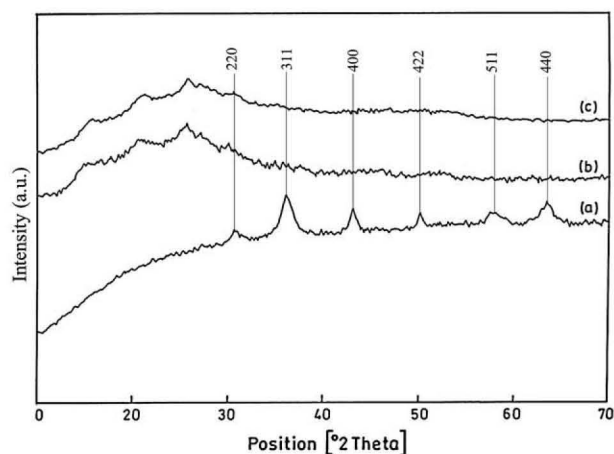


Fig. 1. XRD patterns of (a) $\text{Co}_{0.5}\text{Zn}_{0.5}\text{Fe}_2\text{O}_4$ ferrite nanocrystals, (b) PANI nanofibers and (c) $\text{Co}_{0.5}\text{Zn}_{0.5}\text{Fe}_2\text{O}_4/\text{PANI}$ nanocomposites obtained from reverse microemulsion.

$\text{Co}_{0.5}\text{Zn}_{0.5}\text{Fe}_2\text{O}_4/\text{PANI}$ nanocomposites indicating the fibrous structure. This observation was further corroborated by TEM studies.

Fig. 2a shows the representative TEM image of the ferrite nanocrystals obtained from reverse microemulsion process, which makes the particle size distribution narrower and monodispersed with average diameter of 6 nm.

The representative TEM micrographs of PANI nanostructures obtained via reverse microemulsion process with CTAB are composed of fibrous structures having an average diameter of 20 nm, Fig. 2b. The length of the fibers ranges up to several micrometers.

$\text{Co}_{0.5}\text{Zn}_{0.5}\text{Fe}_2\text{O}_4/\text{PANI}$ nanocomposites were separated by centrifugation; therefore the nanocomposites take the form of round clusters

under the action of centrifugal force, Fig. 2c. The samples were left for few days in distilled water before TEM analysis. TEM image reveals the onset of nanocomposite segregation. Fig. 2d shows a fiber bridging two regions of fragmented nanofiber clusters of the composite. In presence of water the strong H-bonding of PANI fibers with water lessens the force between the clusters leading to segregated nanofibers, Fig. 2d. Further aging in distilled water completely segregates nanocomposites cluster into nanofibers accompanied by vis-à-vis alignment of $\text{Co}_{0.5}\text{Zn}_{0.5}\text{Fe}_2\text{O}_4$ nanocrystals, Fig. 2e and f. TEM micrograph reveals the $\text{Co}_{0.5}\text{Zn}_{0.5}\text{Fe}_2\text{O}_4$ ferrite nanocrystals supported on nanofibrillar PANI having a bimodal size distribution with particles in the 20 nm regime and additional particles roughly 5–

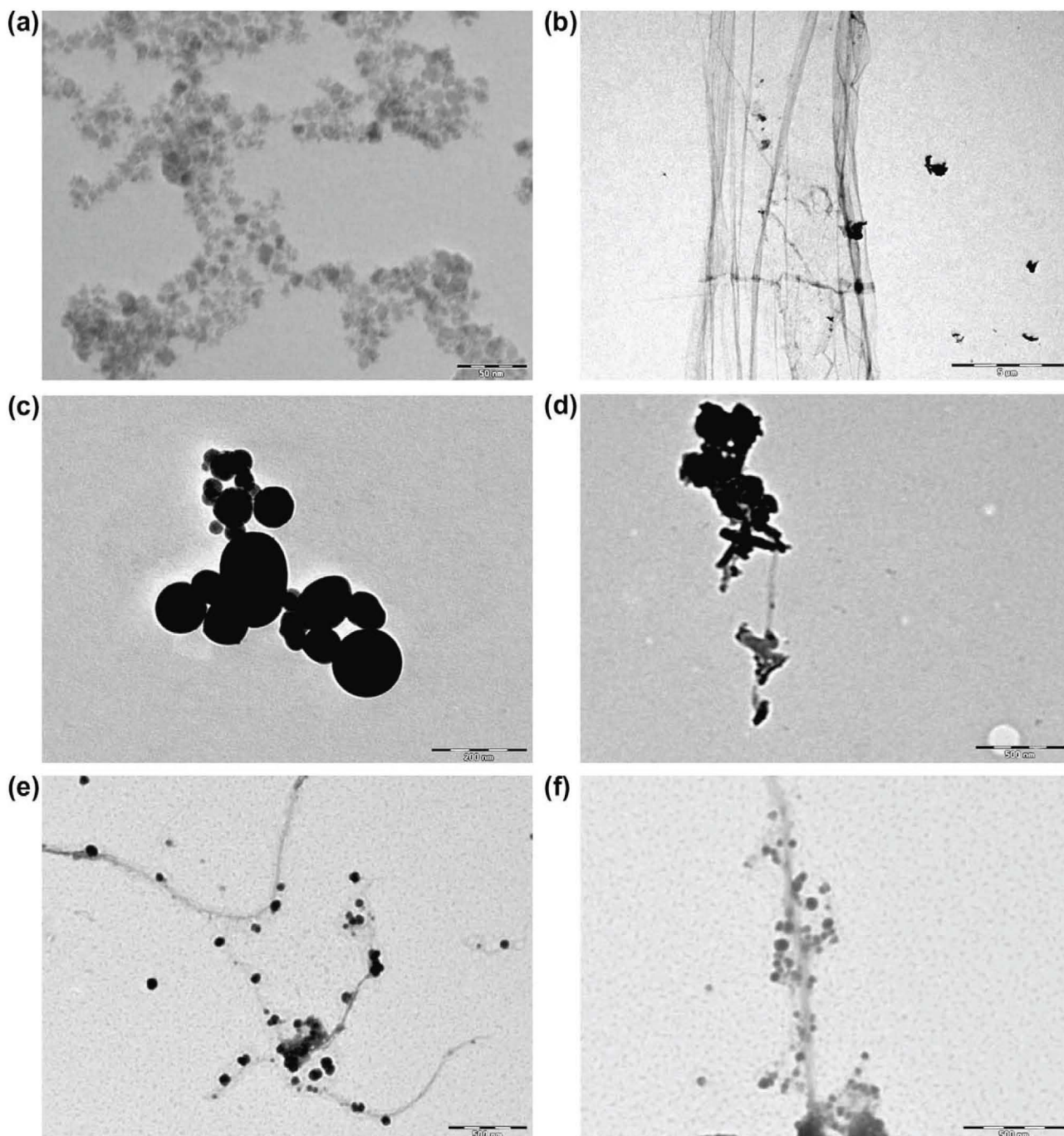


Fig. 2. TEM images of (a) $\text{Co}_{0.5}\text{Zn}_{0.5}\text{Fe}_2\text{O}_4$ ferrite nanocrystals, (b) PANI nanofibers, (c) and (d) clusters of $\text{Co}_{0.5}\text{Zn}_{0.5}\text{Fe}_2\text{O}_4$ ferrite/PANI nanocomposite, (e) and (f) $\text{Co}_{0.5}\text{Zn}_{0.5}\text{Fe}_2\text{O}_4$ ferrite/PANI nanocomposite.

6 nm in diameter. The nanosize ferrite crystals are clearly visible near the border of the nanofiber with ferrite nanocrystals aligned vis-à-vis polyaniline nanofiber.

3.2. Magnetic properties

The room temperature hysteresis loop of all the samples was measured using vibrating sample magnetometer (VSM). Fig. 3 shows their magnetization curves taken at room temperature (300 K). Typical 'S' - like shape of hysteresis loops have been observed, indicating a superparamagnetic property of the synthesized $\text{Co}_{0.5}\text{Zn}_{0.5}\text{Fe}_2\text{O}_4$ ferrite nanocrystals (Fig. 3a). It has been found that the hysteresis loop of $\text{Co}_{0.5}\text{Zn}_{0.5}\text{Fe}_2\text{O}_4$ ferrite nanocrystals could not be saturated with the available maximum field. The hysteresis curve recorded at room temperature for $\text{Co}_{0.5}\text{Zn}_{0.5}\text{Fe}_2\text{O}_4$ ferrite nanocrystals exhibit negligible coercivity and very low remanence, which would be expected from these smaller size particles. This proves that the particles obtained from reverse microemulsion were superparamagnetic at room temperature [34,35].

The magnetic hysteresis loop of $\text{Co}_{0.5}\text{Zn}_{0.5}\text{Fe}_2\text{O}_4$ ferrite/PANI nanocomposite at room temperature is depicted in Fig. 3b. The magnetic properties were inherited from the magnetic $\text{Co}_{0.5}\text{Zn}_{0.5}\text{Fe}_2\text{O}_4$ ferrite nanocrystals. The hysteresis loop for the nanocomposite gets saturated with the available maximum field indicating their ferromagnetic behavior. The saturation magnetization value of bimodal $\text{Co}_{0.5}\text{Zn}_{0.5}\text{Fe}_2\text{O}_4$ ferrite/PANI nanocomposite

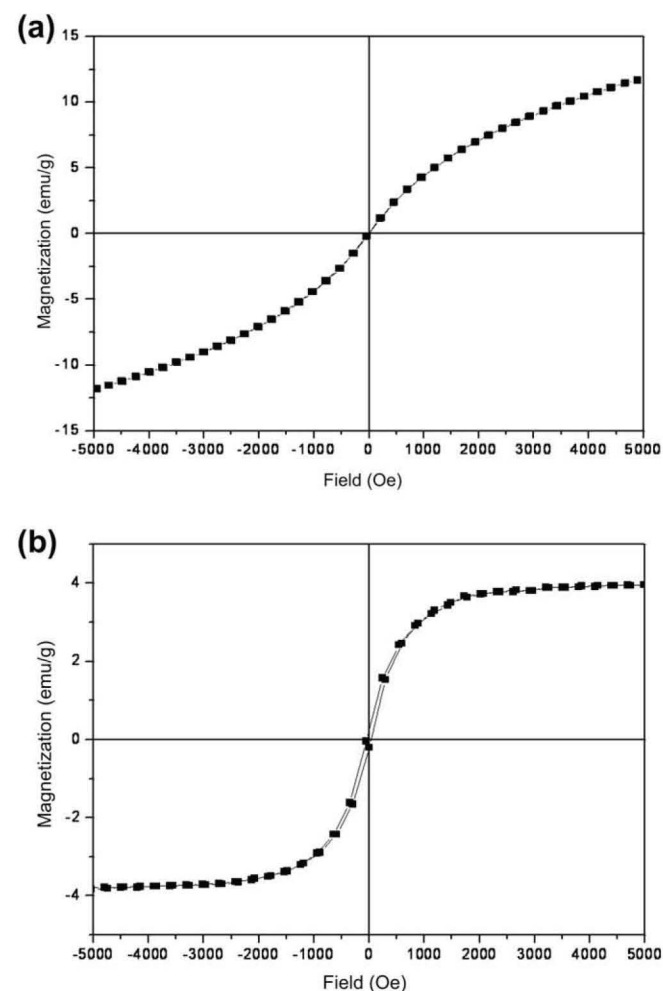


Fig. 3. The hysteresis loops of (a) $\text{Co}_{0.5}\text{Zn}_{0.5}\text{Fe}_2\text{O}_4$ ferrite nanocrystals and (b) $\text{Co}_{0.5}\text{Zn}_{0.5}\text{Fe}_2\text{O}_4$ /PANI nanocomposite obtained from reverse microemulsion measured at 300 K.

was found to be 3.95 emu/g at 300 K with low coercive force (39 Oe). The interactions between the polymer and ferrite nanocrystals play a significant role in attaining the magnetic nature of these composites. The interaction between PANI nanofiber and $\text{Co}_{0.5}\text{Zn}_{0.5}\text{Fe}_2\text{O}_4$ ferrite increases, may be due to H-bonding between -O- of ferrite and hydrogen of -N- of PANI nanofiber. Nanofiber has perfect geometrical orientation for strong H-bonding. Thus increased interactions between polymer and ferrite nanocrystals decrease the particle-particle exchange interaction due to which ferrite nanocrystals aligned in applied magnetic field direction with PANI nanofiber effectively and $\text{Co}_{0.5}\text{Zn}_{0.5}\text{Fe}_2\text{O}_4$ ferrite/PANI became ferromagnetic despite $\text{Co}_{0.5}\text{Zn}_{0.5}\text{Fe}_2\text{O}_4$ ferrite being superparamagnetic.

3.3. Spectral analysis

A typical FTIR spectrum of $\text{Co}_{0.5}\text{Zn}_{0.5}\text{Fe}_2\text{O}_4$ ferrite nanocrystals obtained from reverse microemulsion is shown in Fig. 4a. The FTIR spectra of $\text{Co}_{0.5}\text{Zn}_{0.5}\text{Fe}_2\text{O}_4$ ferrite nanocrystals exhibits a peak at 3444 cm^{-1} attributed to stretching vibrations of hydrogen-bonded surface water molecules and hydroxyl groups [36–38]. Two different sublattices are situated in ferrites metal ions, designated as tetrahedral and octahedral according to the geometrical configuration of the oxygen nearest neighbor atoms. It is believed that the higher frequency band ν_1 i.e., around $580\text{--}600\text{ cm}^{-1}$ is attributed to the intrinsic vibration of the tetrahedral sites and low frequency band ν_1 around $440\text{--}410\text{ cm}^{-1}$ is ascribed to the intrinsic vibration of the octahedral sites [37–39]. FTIR spectra of the prepared ferrite nanocrystals reveals the characteristic peak around 580 and 420 cm^{-1} ascribed to the intrinsic vibration of the tetrahedral and octahedral sites, respectively.

FTIR spectrum confirms the formation of polyaniline (PANI), Fig. 4b. Spectra are consistent with the emeraldine form of polyaniline. The absorption band around 3500 cm^{-1} corresponds to the free N-H bond [40]. The absorption bands at 1580 and 1495 cm^{-1} corresponds to C=C stretching vibrations of the quinoid (N=Q=N) and benzenoid (N-B-N) rings, respectively [40,41]. A shoulder band appears around 1650 cm^{-1} is assigned to the carbonyl group (C=O) indicating the formation of quinone during polymerization [42]. The band at 1495 cm^{-1} can be attributed to aromatic stretching vibrations. Bands at 1364 and 1300 cm^{-1} are attributed to C-N stretching vibrations (41).

Fig. 4c shows the FTIR spectrum of $\text{Co}_{0.5}\text{Zn}_{0.5}\text{Fe}_2\text{O}_4$ ferrite/PANI nanocomposite. The peak intensities in the spectrum of $\text{Co}_{0.5}\text{Zn}_{0.5}\text{Fe}_2\text{O}_4$ ferrite/PANI nanocomposite are similar to the individual

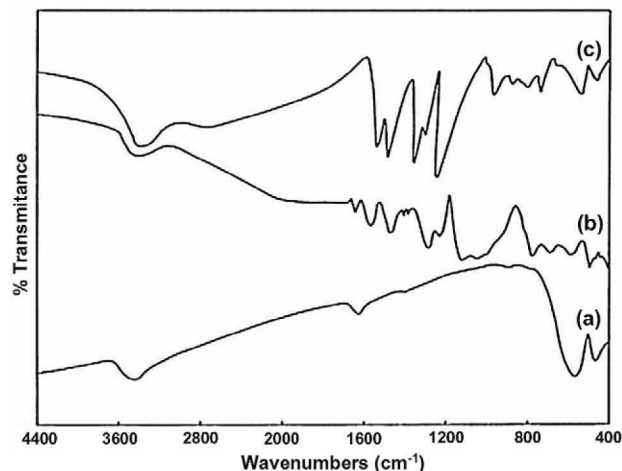


Fig. 4. FTIR spectra of (a) $\text{Co}_{0.5}\text{Zn}_{0.5}\text{Fe}_2\text{O}_4$ ferrite nanocrystals, (b) PANI nanofibers and (c) $\text{Co}_{0.5}\text{Zn}_{0.5}\text{Fe}_2\text{O}_4$ ferrite/PANI nanocomposite.

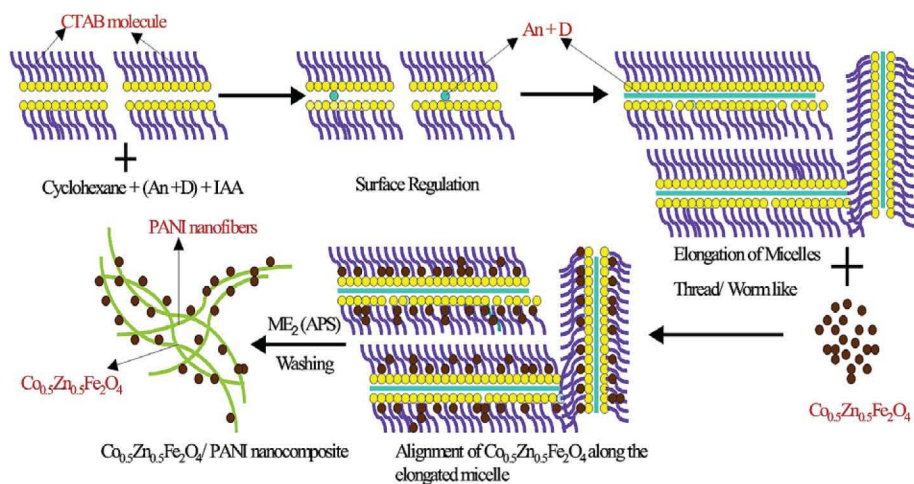


Fig. 5. Schematic illustration of the synthesis process of $\text{Co}_{0.5}\text{Zn}_{0.5}\text{Fe}_2\text{O}_4/\text{PANI}$ nanocomposite. * An: aniline; D: dopant; IAA: iso-amyl alcohol, APS: ammonium per-sulphate.

spectra of $\text{Co}_{0.5}\text{Zn}_{0.5}\text{Fe}_2\text{O}_4$ ferrite and pure PANI. The strong peak intensities of both, i.e. ferrite nanocrystals as well as PANI nanofibers suggest that the $\text{Co}_{0.5}\text{Zn}_{0.5}\text{Fe}_2\text{O}_4$ ferrite nanocrystals are not encapsulated in the PANI shell.

3.4. Self-organization of $\text{Co}_{0.5}\text{Zn}_{0.5}\text{Fe}_2\text{O}_4/\text{PANI}$ nanocomposites

Precisely size regulated magnetic particles are essential to control the alignment of $\text{Co}_{0.5}\text{Zn}_{0.5}\text{Fe}_2\text{O}_4$ ferrite nanocrystals along the PANI nanofiber. Here, we employed reverse microemulsion method to prepare very fine (6 nm) and monodisperse nanocrystals. These $\text{Co}_{0.5}\text{Zn}_{0.5}\text{Fe}_2\text{O}_4$ ferrite nanocrystals retain superparamagnetic behavior at room temperature. Therefore, these $\text{Co}_{0.5}\text{Zn}_{0.5}\text{Fe}_2\text{O}_4$ ferrite nanocrystals are the most suitable for linear alignment along the boundary of the extremely fine PANI nanofibers.

The synthetic procedure for $\text{Co}_{0.5}\text{Zn}_{0.5}\text{Fe}_2\text{O}_4/\text{PANI}$ nanocomposites is schematically illustrated in Fig. 5. The energies of reverse micelle molecules collide and congregate are by far larger than that of the reverse micelle molecules self-organize to regular structure. The reverse micelle molecules assembled parallel just like threads and the growth of particles is limited in these threads like micelles. The thread like or giant worm like micelles represent an extreme case of growth into elongated micelles [43]. Thus, the particles do not aggregate disorderly but self-organized to fiber like elongated micelles to maintain thermal equilibrium of the system. The non-polar solvent cyclohexane weakens the van der Waals and hydrogen bonding interactions between the surfactant molecules, which results in the elongation of the micelle taking the shape of a long fiber. The superparamagnetic $\text{Co}_{0.5}\text{Zn}_{0.5}\text{Fe}_2\text{O}_4$ ferrite nanocrystals have been added to the reverse microemulsion consisting of monomer aniline. These nanocrystals get aligned along the thread like micelles of CTAB instead of entering into the aqueous micelle core. As the reaction proceeds long PANI nanofibers were obtained with $\text{Co}_{0.5}\text{Zn}_{0.5}\text{Fe}_2\text{O}_4$ ferrite nanocrystals aligned vis-à-vis on their surface.

4. Conclusion

In the present work we endeavor a facile synthetic approach for the synthesis of $\text{Co}_{0.5}\text{Zn}_{0.5}\text{Fe}_2\text{O}_4$ ferrite nanocrystals, PANI nanofibers and bifunctional (bimodal) $\text{Co}_{0.5}\text{Zn}_{0.5}\text{Fe}_2\text{O}_4/\text{PANI}$ nanocomposites. This work would result in a synthetic strategy for obtaining morphologically controlled $\text{Co}_{0.5}\text{Zn}_{0.5}\text{Fe}_2\text{O}_4/\text{PANI}$ nanocomposites. Highly superparamagnetic $\text{Co}_{0.5}\text{Zn}_{0.5}\text{Fe}_2\text{O}_4$ ferrite nanocrystals were synthesized by reverse microemulsion route

with an average diameter of 6 nm. Extremely fine PANI nanofibers having an average diameter of 20 nm were synthesized. The length of these fibers range up to several micrometers. Bifunctional $\text{Co}_{0.5}\text{Zn}_{0.5}\text{Fe}_2\text{O}_4/\text{PANI}$ nanocomposites had bimodal size distribution with PANI fibers in the 20 nm regime and additional ferrite crystals 6 nm in diameter. These nanocomposites possess ferromagnetic behavior at room temperature. The present method could be extended for the fabrication of many more nanocomposites with bimodal size distribution, having applications in catalysts supports, biomedical areas or electrical and magnetic shielding.

References

- [1] Trivedi DC. In: Nalwa HS, editor. Handbook of organic conductive molecule and polymers, vol. 2. Chichester: Wiley; 1997. p. 505–72.
- [2] Wei Z, Zhang Z, Wan M. Formation mechanism of self-assembled polyaniline micro/nanotubes. *Langmuir* 2002;18(3):917–21.
- [3] Sun X, Dong S, Wang E. Large scale, templateless, surfactantless route to rapid synthesis of uniform poly (*o*-phenylenediamine) nanobelts. *Chem Commun* 2004:1182–3.
- [4] Huang J, Kaner RB. A general chemical route to polyaniline nanofibers. *J Am Chem Soc* 2004;126(3):851–5.
- [5] Huang J, Kaner RB. Nanofiber formation in the chemical polymerization of aniline: a mechanistic study. *Angew Chem Int Ed* 2004;43(43):5817–21.
- [6] Wu CG, Bein T. Conducting polyaniline filaments in a mesoporous channel host. *Science* 1994;264(5166):1757–9.
- [7] Janata J, Josowicz M. Conducting polymers in electronic chemical sensors. *Nat Mater* 2003;2(1):19–24.
- [8] Naarmann H. Science and application of conducting polymers. Bristol: Adam Hilger; 1991.
- [9] Alivisatos AP. Semiconductor clusters, nanocrystals, and quantum dots. *Science* 1996;271(5251):933–7.
- [10] Sun S, Murray CB, Weller D, Folks L, Moser A. Monodisperse FePt nanoparticles and ferromagnetic FePt nanocrystal superlattices. *Science* 2000;287(5460):1989–92.
- [11] Redl FX, Cho K-S, Murray CB, O'Brien S. Three-dimensional binary superlattices of magnetic nanocrystals and semiconductor quantum dots. *Nature* 2003;423(6943):968–71.
- [12] Park J, Joo J, Kwon S, Jang Y, Hyeon T. Synthesis of monodisperse spherical nanocrystals. *Angew Chem Int Ed* 2007;46(25):4630–60.
- [13] Deng JG, He CL, Peng YX, Wang JH, Long XP, Li P, et al. Magnetic and conductive Fe_3O_4 polyaniline nanoparticles with core-shell structure. *Synthetic Metals* 2003;139(2):295–301.
- [14] Wan MX, Li WC. A composite of polyaniline with both conducting and ferromagnetic functions. *J Polym Sci Part A: Polym Chem* 1997;35(11):2129–36.
- [15] Zhang Z, Wan M. Nanostructures of polyaniline composites containing nanomagnet. *Synthetic Metals* 2003;132(2):205–12.
- [16] Gomez-Romero P. Hybrid organic-inorganic materials – in search of synergic activity. *Adv Mater* 2001;13(3):163–74.
- [17] Sazou D. Electrodeposition of ring-substituted polyanilines on Fe surfaces from aqueous oxalic acid solutions and corrosion protection of Fe. *Synthetic Metals* 2001;118(1–3):133–47.
- [18] Sunderland K, Brunetti P, Spinu L, Fang J, Wang Z, Lu W. Synthesis of g- $\text{Fe}_2\text{O}_3/\text{polypyrrole}$ nanocomposite materials. *Mater Lett* 2004;58(25):3136–40.

- [19] Jarjayes O, Fries PH, Bidan C. New nanocomposites of polypyrrole including γ - Fe_2O_3 particles: electrical and magnetic characterizations. *Synthetic Metals* 1995;69(1-3):343-4.
- [20] Yan F, Xue G, Chen J, Lu Y. Preparation of a conducting polymer/ferromagnet composite film by anodic-oxidation method. *Synthetic Metals* 2001;123(1):17-20.
- [21] Wu KH, Shin YM, Yang CC, Ho WD, Hsu JS. Preparation and ferromagnetic properties of $\text{Ni}_{0.5}\text{Zn}_{0.5}\text{Fe}_2\text{O}_4$ /polyaniline core-shell nanocomposites. *J Polym Sci Part A: Polym Chem* 2006;44(8):2657-64.
- [22] Xie G, Zhang Q, Luo Z, Wu M, Li T. Preparation and characterization of monodisperse magnetic poly (styrene butyl acrylate methacrylic acid) microspheres in the presence of a polar solvent. *J Appl Polym Sci* 2003;87(11):1733-8.
- [23] Alam J, Riaz U, Ahmad S. Effect of ferrofluid concentration on electrical and magnetic properties of the Fe_3O_4 /PANI nanocomposites. *J Magn Magn Mater* 2007;314(2):93-9.
- [24] Bao L, Jiang JS. Evolution of microstructure and phase of Fe_3O_4 in system of Fe_3O_4 polyaniline during high-energy ball milling. *Phys B: Phys Condens Matter* 2005;367:182-7.
- [25] Xuan S, Wang Y-XJ, Leung KCF, Shu K. Synthesis of Fe_3O_4 @polyaniline core/shell microspheres with well-defined blackberry-like morphology. *J Phys Chem C* 2008;112(48):18804-9.
- [26] Zhong-ai H, Hong-Xiao Z, Chao K, Yu-ying Y, Xiu-li S, Li-jun R, et al. The preparation and characterization of quadrate NiFe_2O_4 /polyaniline nanocomposites. *J Mater Sci: Mater Electron* 2006;17(11):859-63.
- [27] Vaidyanathan G, Sendhilnathan S, Arulmurgan R. Structural and magnetic properties of $\text{Co}_{1-x}\text{Zn}_x\text{Fe}_2\text{O}_4$ nanoparticles by co-precipitation method. *J Magn Magn Mater* 2007;313(2):293-9.
- [28] Caizer C, Stefanescu M. Magnetic characterization of nanocrystalline Ni-Zn ferrite powder prepared by the glyoxylate precursor method. *J Phys D* 2002;35:3035-40.
- [29] Dong C. *PowderX*: windows-95-based program for powder X-ray diffraction data processing. *J Appl Crystallogr* 1999;32:838.
- [30] Gao HX, Jiang T, Han BX, Wang Y, Du JM, Liu ZM, et al. Aqueous/ionic liquid interfacial polymerization for preparing polyaniline nanoparticles. *Polymer* 2004;45(9):3017-9.
- [31] Luzny W, Sniechowski M, Laska J. Structural properties of emeraldine base and the role of water contents: X-ray diffraction and computer modelling study. *Synthetic Metals* 2002;126(1):27-35.
- [32] Pouget JP, Josefowicz ME, Epstein AJ, Tang X, Mac Diarmid AG. X-ray structure of polyaniline. *Macromolecules* 1991;24(3):779-89.
- [33] Yavuz O, Ram MK, Aldissi M, Poddar P, Hariharan S. Synthesis and the physical properties of MnZn ferrite and NiMnZn ferrite-polyaniline nanocomposite particles. *J Mater Chem* 2005;15:810-7.
- [34] Upadhayay T, Upadhayay RV, Mehta RV. Characterization of a temperature-sensitive magnetic fluid. *Phys Rev B* 1997;55(9):5585-8.
- [35] Xaun S, Hao L, Jiang W, Gong X, Hu Y, Chen Z. Preparation of water-soluble magnetite nanocrystals through hydrothermal approach. *J Magn Magn Mater* 2007;308(2):210-3.
- [36] Dallas P, Stamopoulos D, Boukos N, Tzitzios V, Niarchos D, Petridis D. Characterization, magnetic and transport properties of polyaniline synthesized through interfacial polymerization. *Polymer* 2007;48(11):3162-9.
- [37] Garcia-Cerda LA, Montemayor SM. Synthesis of CoFe_2O_4 nanoparticles embedded in a silica matrix by the citrate precursor technique. *J Magn Magn Mater* 2005;294(2):e43-6.
- [38] Ahn Y, Choi EJ, Kim EH. Superparamagnetic relaxation in cobalt ferrite nanoparticles synthesized from hydroxide carbonate precursors. *Rev Adv Mater Sci* 2003;5:477-80.
- [39] Wu N, Fu L, Su M, Aslam M, Wong KC, Dravid VP. Interaction of fatty acid monolayers with cobalt nanoparticles. *Nano Lett* 2004;4:383-6.
- [40] Stejskal J, Sapurina I, Trchova M, Konyushenko EN, Holler P. The genesis of polyaniline nanotubes. *Polymer* 2006;47(25):8253-62.
- [41] Konyushenko EN, Stejskal J, Sedenkova I, Trchova M, Sapurina I, Cieslar M, et al. Polyaniline nanotubes: the conditions of formation. *Polym Int* 2006;55(1):31-9.
- [42] Landfester K. Miniemulsions for nanoparticle synthesis. *Topics in current chemistry: colloid chemistry II*, vol. 227. Berlin/Heidelberg: Springer; 2003. p. 75-123.
- [43] Bernheim-Groswasser A, Zana R, Talmon Y. Sphere-to-cylinder transition in aqueous micellar solution of a dimeric (Gemini) surfactant. *J Phys Chem B* 2000;104(17):4005-9.